[3] Leitmann, G., "Note on 'Establishment of a circular satellite orbit by double impulse,'" J. Brit. Interplanet. Soc. **17**, 358–359 (1960).

[4] Jantscher, H. N., Olson, D. ,and Saari, A. E., "Minimum energy analysis for the general problem of rendezvous in earth orbital space," ARS J. **32**, 292–294 (1962).

[5] Moulton, F. R., *Celestial Mechanics* (Macmillan Co., New York, 1914).

[6] Barnes, S. W., "Elliptical trajectories," General Electric TIS Ser. R57EMH31, General Electric Co., Electronics Div., Syracuse, N. Y. (June 1957).

JUNE 1963 AIAA JOURNAL VOL. 1, NO. 6

Design Analysis of Earth-Lunar Trajectories: Launch and Transfer Characteristics

J. E. MICHAELS*
Northrop Corporation, Hawthorne, Calif.

In the design of feasible Earth-lunar trajectories, the launch or boost phase must be linked realistically to the ballistic phase within certain well-defined constraints. This paper presents the relationships between the pertinent parameters from launch to arrival in graphical form which not only are useful in the design of lunar trajectories but also are effective aids in the visualization of the problem's fundamentals. The analysis covers all possible ballistic trajectories to the moon, including lofted trajectories, in as simple a form as is believed possible. The method also is applicable to return trajectories by a simple time reversal technique such that predetermined Earth arrival conditions are assured.

Nomenclature

a = semimajor axis of transfer orbit
A_L = launch azimuth angle (clockwise from local north)
e = eccentricity of transfer orbit
i = inclination of transfer orbital plane to equator
$\mathbf{L}$ = unit vector toward launch site at time of launch
r_1 = radius vector at injection, 4078.2860 statute miles (100-naut-mile alt)
r_2 = radius vector at arrival (mean moon distance of 60.27 Earth radii)
$\mathbf{S}$ = unit vector toward moon at time of arrival
t_L = hours from midnight to launch time of launch day
T = total flight time (launch to arrival)
T_b = ballistic flight time (injection to arrival)
T_p = powered plus parking orbit flight time (launch to injection)
v_1 = true anomaly at injection
v_2 = true anomaly at arrival
V = injection velocity
V_{cir} = circular velocity at 100-naut-mile alt (25,568 fps)
$\mathbf{W}$ = unit vector normal to plane of transfer orbit
α_L = right ascension of L
α_S = right ascension of S
γ = angle of elevation at injection
δ_L = declination of L
δ_S = declination of S
θ_L = longitude of launch site (positive eastward from Greenwich)
μ_e = gravitational constant of Earth, 9.5629993×10^4 statute miles^3/sec^2
φ = total central angle (launch to arrival)
φ_b = ballistic central angle (injection to arrival)
φ_p = powered plus parking orbit central angle (launch to injection)
ω = angular velocity of Earth's rotation (15.04107 deg/hr)
ω_{100} = angular velocity in 100-naut-mile circular orbit (244.91 deg/hr)
GHA = Greenwich hour angle of vernal equinox at 0^h UT of launch day
(All times are given as Universal Time (UT) unless otherwise noted.)

Presented at the IAS National Summer Meeting, Los Angeles, Calif., June 19–22, 1962; revision received April 5, 1963.

* Formerly Supervisor, Space Mechanics, Norair Division; presently Head, Trajectory Analysis Section, Systems Research and Planning Division, Aerospace Corporation, Los Angeles, Calif.

1. Introduction

IN the design of actual hardware for lunar flights, realistic trajectories must be considered for detailed analysis. Although general information about lunar trajectories such as is given in Refs. 1–4 is helpful, the problem of selecting realistic trajectories involves the integration of many widely differing constraints, originating from various sources, which actually may dictate the class of trajectories which can be considered for a particular mission. Many of these constraints are associated with the geometry and dynamics at launch. Therefore, this paper is concerned with those parameters that define launch and ballistic transfer into the vicinity of the moon.

Following the method of Clarke,[5] the problem is divided into two main parts: the geometric constraints that control the plane of the transfer trajectory, and the dynamic constraints that determine the motion in that plane. Although the mathematics is straightforward, the geometry is sufficiently complex to make desirable the aids in visualization presented herein such that the physical significance of the various parameters is made as clear as possible.

2. Geometric Constraints

Consider two unit vectors with origin at the Earth's center: a launch vector **L** in the direction of the launch site at the time of launch, and an outward radial vector **S** in the direction of the moon at the time of arrival. These two vectors define a fixed plane in space which is the plane of the transfer trajectory. This plane forms an angle with the local north at the launch site and time which is the launch azimuth angle A_L. The angle between these vectors is the total central angle φ.

Figure 1a shows these parameters and defines the coordinate system used. In terms of the reference axes shown,

$$\mathbf{L} = i\,L_x + j\,L_y + k\,L_z \tag{1}$$

$$\mathbf{S} = i\,S_x + j\,S_y + k\,S_z \tag{2}$$

where i,j,k are unit vectors in the x,y,z coordinate system and

$$\begin{aligned} S_x &= \cos\alpha_s \cos\delta_s \\ S_y &= \sin\alpha_s \cos\delta_s \\ S_z &= \sin\delta_s \end{aligned} \tag{3}$$

$$\begin{aligned} L_x &= \cos\alpha_L \cos\delta_L \\ L_y &= \sin\alpha_L \cos\delta_L \\ L_z &= \sin\alpha_L \end{aligned} \tag{4}$$

A unit vector $\mathbf{W}$ is introduced perpendicular to the plane of the flight path defining that plane:

$$\mathbf{W} = (\mathbf{L} \times \mathbf{S})/(|\mathbf{L} \times \mathbf{S}|) = i\,W_x + j\,W_y + k\,W_z \tag{5}$$

Now

$$|\mathbf{L} \times \mathbf{S}| = \sin\varphi \tag{6}$$

where φ is the angle between $\mathbf{L}$ and $\mathbf{S} < 180°$. Thus

$$W_z = (L_x S_y - L_y S_x)/\sin\varphi \tag{7}$$

But W_z is the direction cosine of $\mathbf{W}$ with respect to the z axis and is therefore

$$W_z = \cos i \tag{8}$$

By spherical trigonometry, it follows that

$$W_z = \cos i \cos\delta_L \sin A_L \tag{9}$$

Solving Eq. (9) for A_L and using Eq. (7) gives

$$\sin A_L = (L_x S_y - L_y S_x)/\sin\varphi \cos\delta_L \tag{10}$$

All that remains is to express φ in terms of $\mathbf{S}$ and $\mathbf{L}$ which is done easily by taking the scalar product

$$\mathbf{L}\cdot\mathbf{S} = \cos\varphi = L_x S_x + L_y S_y + L_z S_z \tag{11}$$

An expression for A_L not involving the transcendental difficulties of solving for A_L using Eqs. (10) and (11) has been obtained by Kohlhase[6] after following a somewhat different route:

$$\tan A_L = \frac{\sin\alpha_L S_x - \cos\alpha_L S_y}{(\cos\alpha_L S_x + \sin\alpha_L S_y)\sin\delta_L - \cos\delta_L S_z} \tag{12}$$

which with Eq. (10) identifies the correct quadrant for A_L. Both relationships are of use, since φ also must be determined.

Graphical relationships between these parameters are shown in Figs. 2 and 3 for Atlantic Missile Range (AMR) and Pacific Missile Range (PMR) launch sites, respectively. Here, on plots of the outward radial declination δ_s vs the right ascension difference $(\alpha_L - \alpha_s)$, are iso-φ and iso-A_L lines depicting every possible geometric relationship between $\mathbf{L}$ and $\mathbf{S}$. Since $\mathbf{L}$ is taken at launch and $\mathbf{S}$ at arrival, the total trip time T is treated as a variable and together with φ forms the connecting link with the dynamic parameters of the transfer trejectory.

Some remarks should be made concerning Figs. 2 and 3. Each iso-line has two values: uncircled and circled. The uncircled value φ refers to the angle between $\mathbf{L}$ and $\mathbf{S}$ less than 180°. The uncircled value A_L is the launch azimuth angle associated with the uncircled φ, i.e., launch in the direction as $\mathbf{L}$ moves toward $\mathbf{S}$ through the uncircled φ angle. Obviously, a launch in the same plane but in the opposite direction is possible geometrically. Thus a circled value φ, equal to the explement of φ, and a circled A_L, equal to A_L plus π, also exist for every iso-line (see Figs. 1b and 1c). In using the curves, care must be taken to use only uncircled values together or only circled values together.

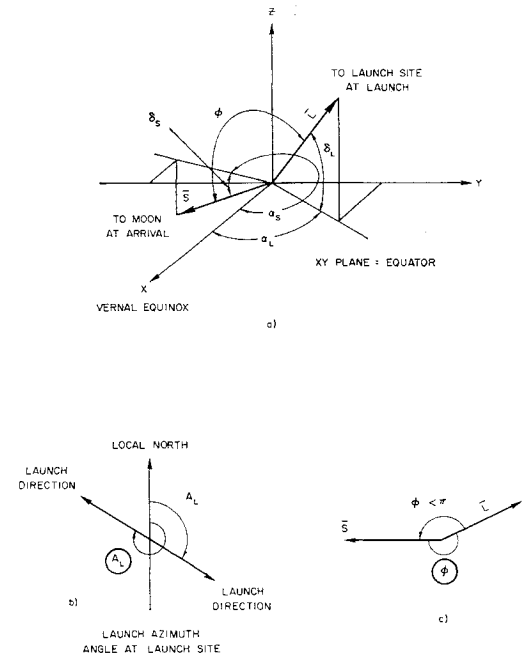

Fig. 1 Geometric parameters

The unshaded areas refer to values of A_L which fall within the launch azimuth safety limits for the particular launch site. For AMR, the launch azimuth safety limits are from 46° to 114°; for PMR, they are from 172° to 300°. Note that there are two unshaded areas in each figure, one referring to uncircled values and the other to circled values of A_L.

The launch time of day is related to α_L by the following:

$$\alpha_L = \text{GHA} + \theta_L + \omega t_L \tag{13}$$

where GHA is the Greenwich hour angle of the vernal equinox at 0^h UT of the launch day, θ_L is the longitude of the launch site (positive eastward), ω is the angular velocity of the Earth (15.04107 deg/hr), and t_L is the hours from midnight to launch time of the launch day.

For a given lunar declination, there exist two values of $(\alpha_L - \alpha_s)$ having a specified launch azimuth A_L. This means that twice daily the plane determined by the $\mathbf{L}$ and $\mathbf{S}$ vectors assumes a given azimuth. The central angle φ for these two cases differs, requiring parking orbit coast periods of different lengths and different points of final injection relative to the Earth's surface. Thus, an option exists which permits the selection of the more favorable launch conditions from these two possibilities daily.

3. Dynamic Constraints

During launch, the vehicle must undergo a boost phase that must be included in the total flight time T and total central angle φ. Thus

$$T = T_p + T_b \tag{14}$$

$$\varphi = \varphi_p + \varphi_b \tag{15}$$

where T_p and φ_p refer to the time and central angle of the boost phase (launch to injection), and T_b and φ_b refer to the ballistic phase (injection to arrival). Note that the boost phase usually will include coast in a parking orbit prior to a final injection into the lunar transfer orbit.

The rest of the dynamic parameters which define the characteristics of the transfer orbit are shown in Fig. 4. Using simple two-body mechanics, the relationships between these parameters are given by the following equations:

$$T_b = T_2 - T_1 \tag{16}$$

$$\varphi_b = v_2 - v_1 \tag{17}$$

$$\gamma = \arctan\left[\frac{e \sin v_1}{1 + e \cos v_1}\right] \tag{18}$$

$$\frac{V}{V_{cir}} = \left[2 - \frac{r_1}{a}\right]^{1/2} \tag{19}$$

where

$$T_1 = \left[\frac{a^3}{\mu_e}\right]^{1/2}(E_1 - e \sin E_1) \qquad T_2 = \left[\frac{a^3}{\mu_e}\right]^{1/2}(E_2 - e \sin E_2)$$

$$E_1 = \arccos\left[\frac{a - r_1}{ae}\right] \qquad E_2 = \arccos\left[\frac{a - r_2}{ae}\right]$$

$$v_1 = \arccos\left[\frac{(a/r_1)(1 - e^2) - 1}{e}\right]$$

$$v_2 = \arccos\left[\frac{(a/r_2)(1 - e^2) - 1}{e}\right]$$

To maximize booster payload capabilities, in theory final injection should occur as close to perigee of the transfer orbit as possible and at as low an altitude as is practical. However, for specific booster stage combinations, deviations from ideal conditions may result because of the complex dynamics of the boost phase. Thus, the boost phase central angle φ_p, the injection angle of elevation γ, and the injection altitude r_1 are characteristics of specific launch hardware. In this analysis φ_p and γ are treated as parameters, whereas r_1 is fixed at 100 naut miles. It has been suggested[5,6] that this injection altitude is a practical minimum. However, the effect of possible variations of r_1 in the results is not significant for the objectives of this paper.

Graphical relationships between these parameters are shown in Fig. 5. Here, on a plot of T_b vs φ_b, are iso-lines of the parameters a, γ, and V/V_{cir}. Four distinct types of transfer orbits are contained within these curves and are defined in Fig. 6. Although Eqs. (16–19) refer only to post-perigee direct transfers, simple conversions of these basic formulas can be made to apply to the other types. A complete discussion of these various transfer modes has been given by Vertregt.[7] Although the area of most interest in Fig. 5 is centered around the $\gamma = 0$ line, a total parametric display often is helpful in understanding the physical significance of a complete range in values of the parameters. Obviously, pre-perigee transfers involving negative values of γ are limited to the region close to the $\gamma = 0$ line since these would require traversing actual perigee altitudes of less than 100 naut miles.

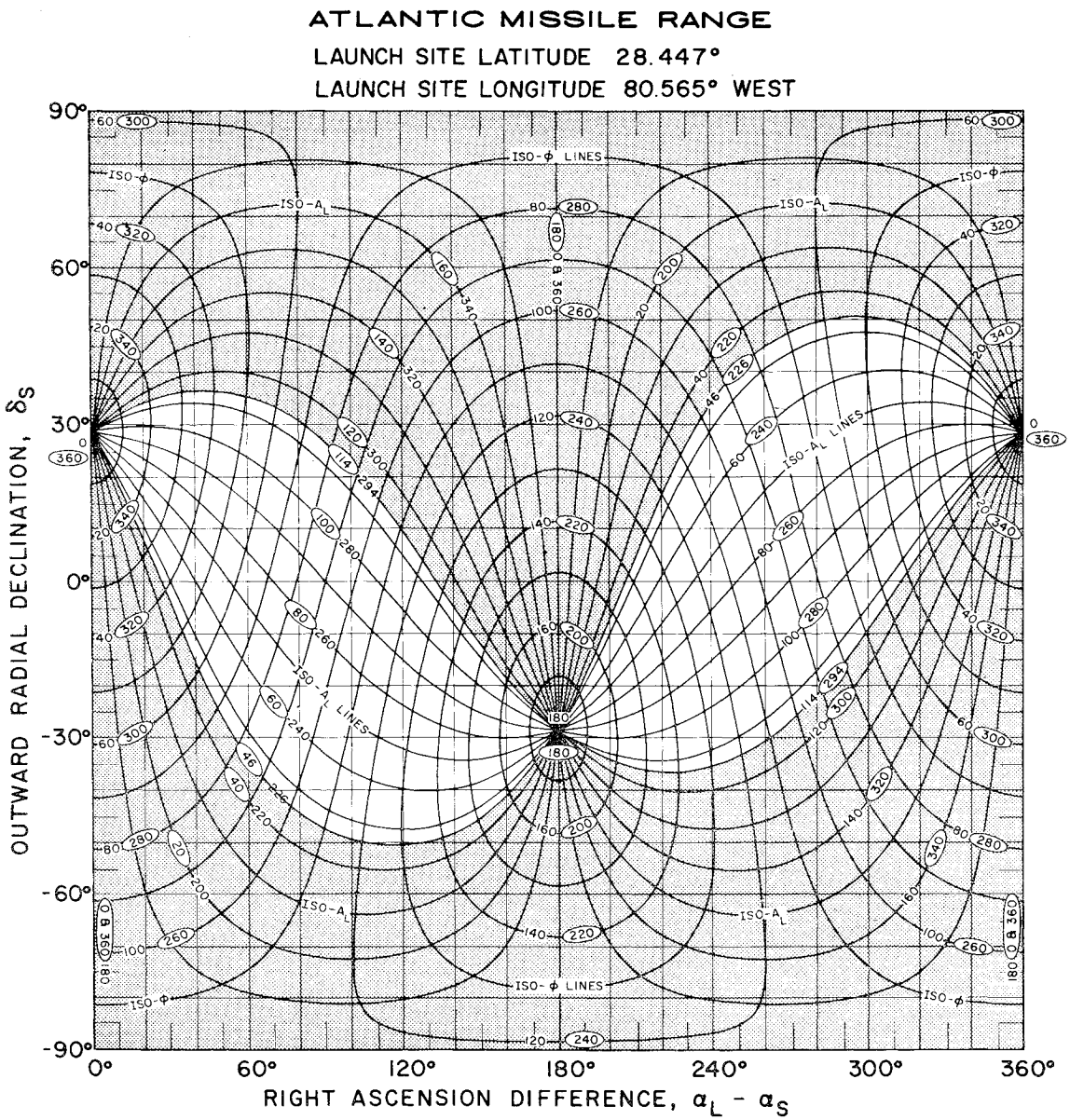

Fig. 2 Iso-φ and iso-A_L contours, AMR launch site

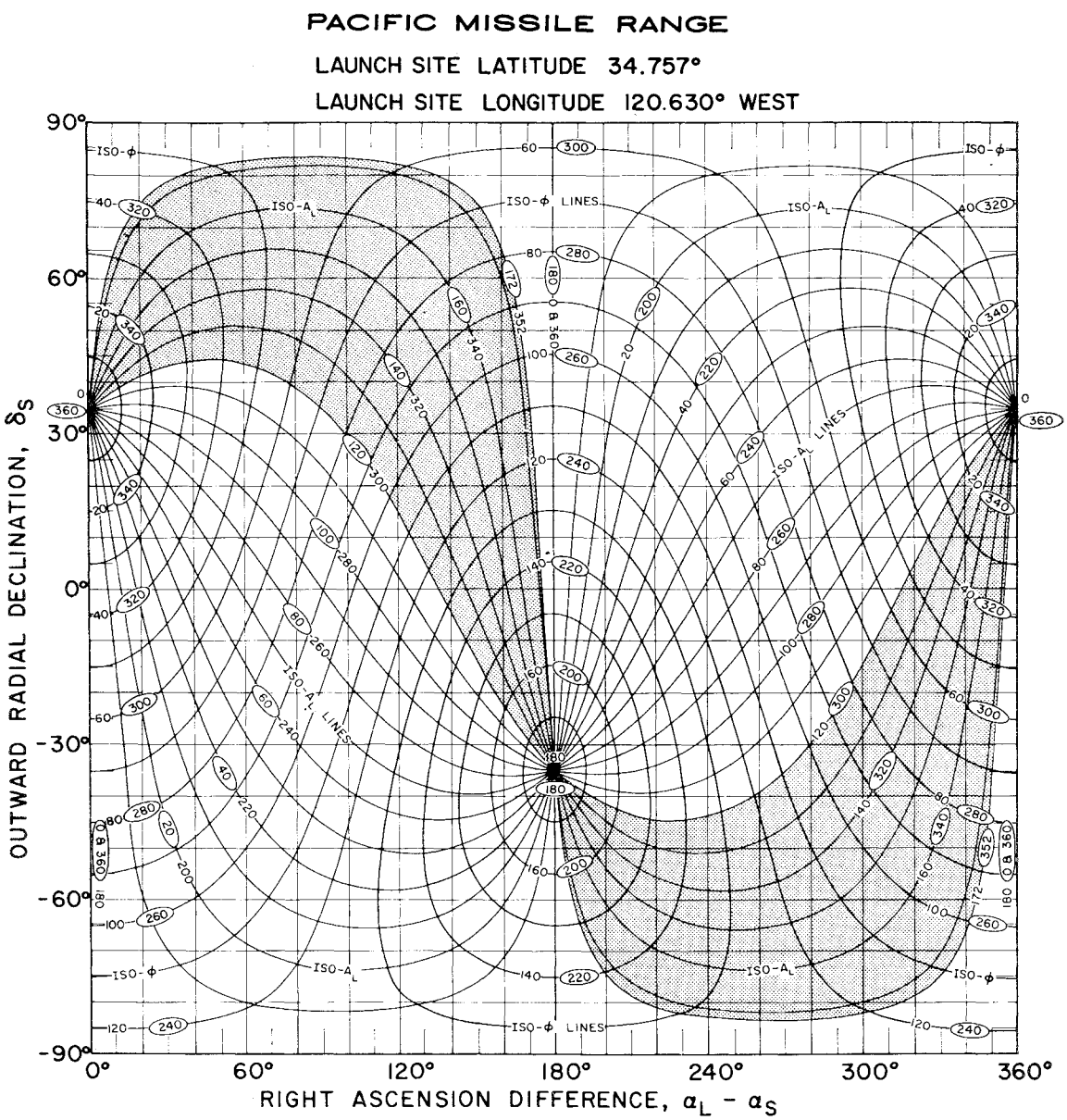

Fig. 3 Iso-φ and iso-A_L contours, PMR launch site

4. Other Constraints

Although the curves of Figs. 2, 3, and 5 present a complete picture of the basic parameters involved, before a specific trajectory can be selected, other constraints may have to be considered for specific lunar missions. One such constraint has to do with tracking station visibility. At the present stage of space flight development, tracking and communication with an unmanned vehicle are essential functions to the post injection guidance problem and the transmission of scientific data. For instance, if only one tracking station has command capability, which must be used during the terminal phase of an unmanned lunar flight, the time of arrival must occur during a period of that tracking station's visibility. Obviously, the separation in longitude between the launch site and the tracking station is involved, as well as the total trip time. Not so obvious is the effect of the amount of coast in a parking orbit prior to injection. The tracking requirement ultimately results in constraints on the total trip time T within certain definite limits.

Another constraint has to do with the lighting of the moon (or its phase) upon arrival. For instance, in the case of an unmanned mission for lunar exploration such as Surveyor, the lighting of the moon is an important factor in the performance of certain scientific experiments. Since many different experiments as well as the reliability of components are involved, time becomes a factor, and an overall requirement might feasibly be to maximize the period of lunar daylight upon arrival. For a given arrival point on the moon, this would specify a particular value of α_s depending upon the time of year.

It should be noted that the constraints discussed so far are of a very practical nature that fairly well dictates the class

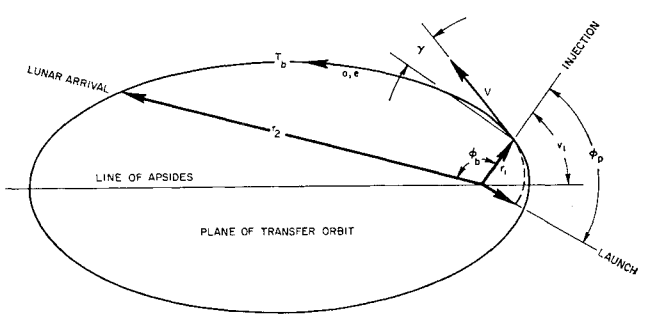

Fig. 4 Dynamic parameters

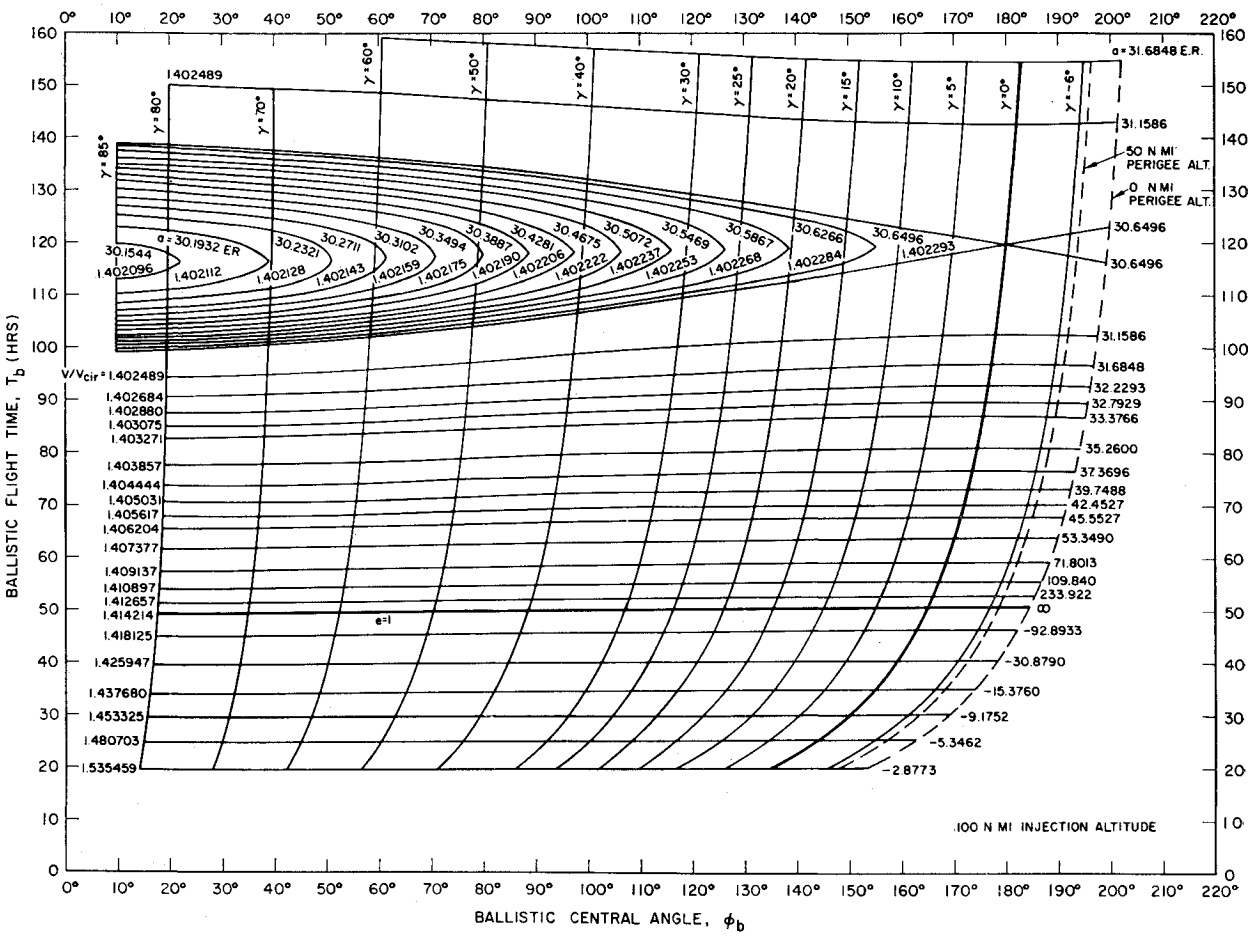

Fig. 5 Display of dynamic parameters

of trajectories which must be considered for the unmanned lunar missions presently under consideration. This does not mean that optimization studies of ideal trajectories based on particular criteria are of little value. It simply means that the realization of such idealized trajectories always will be subject to practical constraints, some of which have been discussed here. For instance, in a manned lunar mission the radiation hazard may impose restrictions on the trajectory such that many desirable factors may have to be ignored completely. No attempt is made here to consider all possible constraints that might influence the selection of a particular lunar trajectory. Rather, the approach is to identify the more basic ones associated with launch and transfer and to demonstrate how they can be integrated into a trajectory selection technique.

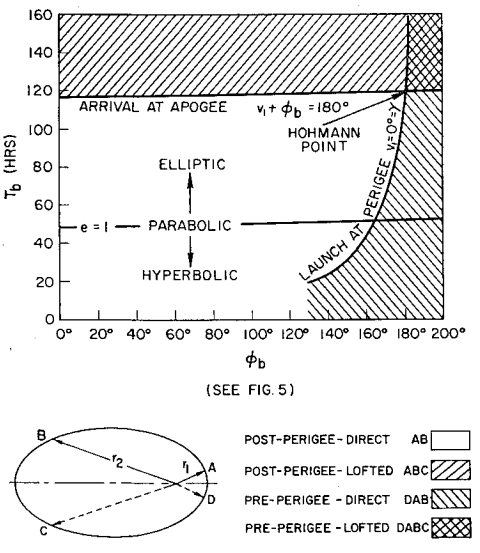

Fig. 6 Types of transfer orbits

5. Trajectory Selection

In the selection of an Earth-lunar trajectory for a specific mission, certain parameters will be known or given. This includes such things as the launch site coordinates and the booster hardware parameters φ_p, T_p, and γ. The launch azimuth angle A_L always is subject to the range safety restrictions. Tracking and communication requirements would establish feasible trip times T, and mission requirements might restrict T further as well as specify the phase of the moon at arrival. In the example that follows, it is assumed that these constraints have been specified, and the problem is to select a compatible trajectory in sufficient detail to serve as a first approximation to a precision trajectory program search.

Example I: Earth-to-Moon Trajectory

Given:

1) AMR launch.

2) $95° \leq A_L \leq 110°$ (A due east launch, $A_L = 90°$, is desirable to maximize the Earth's rotational boost but is not as important as good downrange tracking, which for AMR is between 95° and 110°.)

3) $T_p \geq 0^h27$ (no parking orbit for minimum value).
4) $\varphi_p \geq 40°$ (no parking orbit for minimum value).
5) $\gamma = 0° = v_1$ (perigee injection).
6) $r_1 = 4078$ statute miles (100-naut-mile alt).
7) $T = 64^h00$ (for Goldstone visibility at arrival).
8) Lunar arrival at approximate full phase in September 1961.
9) Minimum coast in parking orbit. (Select from two possibilities daily.)

Solution:

1) $T_b = T - T_p = 64^h00 - 0^h27 = 63^h73$.
2) From Fig. 5, for $\gamma = 0°$ and $T_b = 63^h73$, read $\varphi_b = 170°$.
3) $\varphi_{\min} = \varphi_p + \varphi_b = 40° + 170° = 210°$ (no parking orbit).
4) From Ref. 8 (p. 159), for lunar full phase in September 1961, read 11^h57 (September 24, 1961).
5) From Ref. 8 (p. 134), for lunar arrival at roughly 12^h (September 24, 1961), read $\alpha_s = 2°.50$ and $\delta_s = -2°.14$.
6) From Fig. 2, for $\delta_s = -2°.14$ and $A_L = 95°$, read $(\alpha_L - \alpha_s) = 105°$ and $\varphi = 256°$ (circled values) or $(\alpha_L - \alpha_s) = 276°.5$ and $\varphi = 85°.5$ (uncircled values). Choosing the "uncircled" answers would require a boost plus parking orbit central angle of well over 180°, whereas the "circled" values will require only $256° - 107° = 86°$. Therefore, choose the "circled" values and proceed.
7) Compute: $\alpha_L = (\alpha_L - \alpha_s) + \alpha_s = 105° + 2°.5 = 107°.5$.
8) From Ref. 8 (p. 15), for 0^h (September 21, 1961), the day of launch, read GHA = 359°.63.
9) Compute: $t_L = (\alpha_L - \text{GHA} - \theta_L)/\omega = [107°.5 - 359°.63 - (-80°.57)]/15°.04107 = 12^h53$ (September 21, 1961) launch time.
10) Lunar arrival date-time = 12^h53 (September 21, 1961) + $64^h = 4^h53$ (September 24, 1961).
11) Redetermine α_s from Ref. 8, for better value of arrival time, $\alpha_s = 358°.10$ and $\delta_s = -3°.87$.
12) Again from Fig. 2, for $\delta_s = -3°.87$ and $A_L = 95°$, read $(\alpha_L - \alpha_s) = 108°$ and $\varphi = 252°.5$, with $\varphi_p = 252°.5 - 170° = 82°.5$.
13) Time spent in parking orbit = $(\varphi_p - \varphi_{p\,\min})/\omega_{100} = (82°.5 - 40°)/244°.91 = 0^h17$. Thus $T_b = 64^h00 - 0^h27 - 0^h17 = 63^h56$, with no readable change in φ_b from previous value.
14) Recompute: $\alpha_L = 108° + 358°.10 = 106°.10$ and $t_L = (106°.1 - 359°.63 + 80°.57)/15°.04107 = 12^h44$ (September 21, 1961).
15) New lunar arrival date time = 12^h44 (September 21, 1961) + $64^h = 4^h44$ (September 24, 1961), with $\alpha_s = 358°.04$

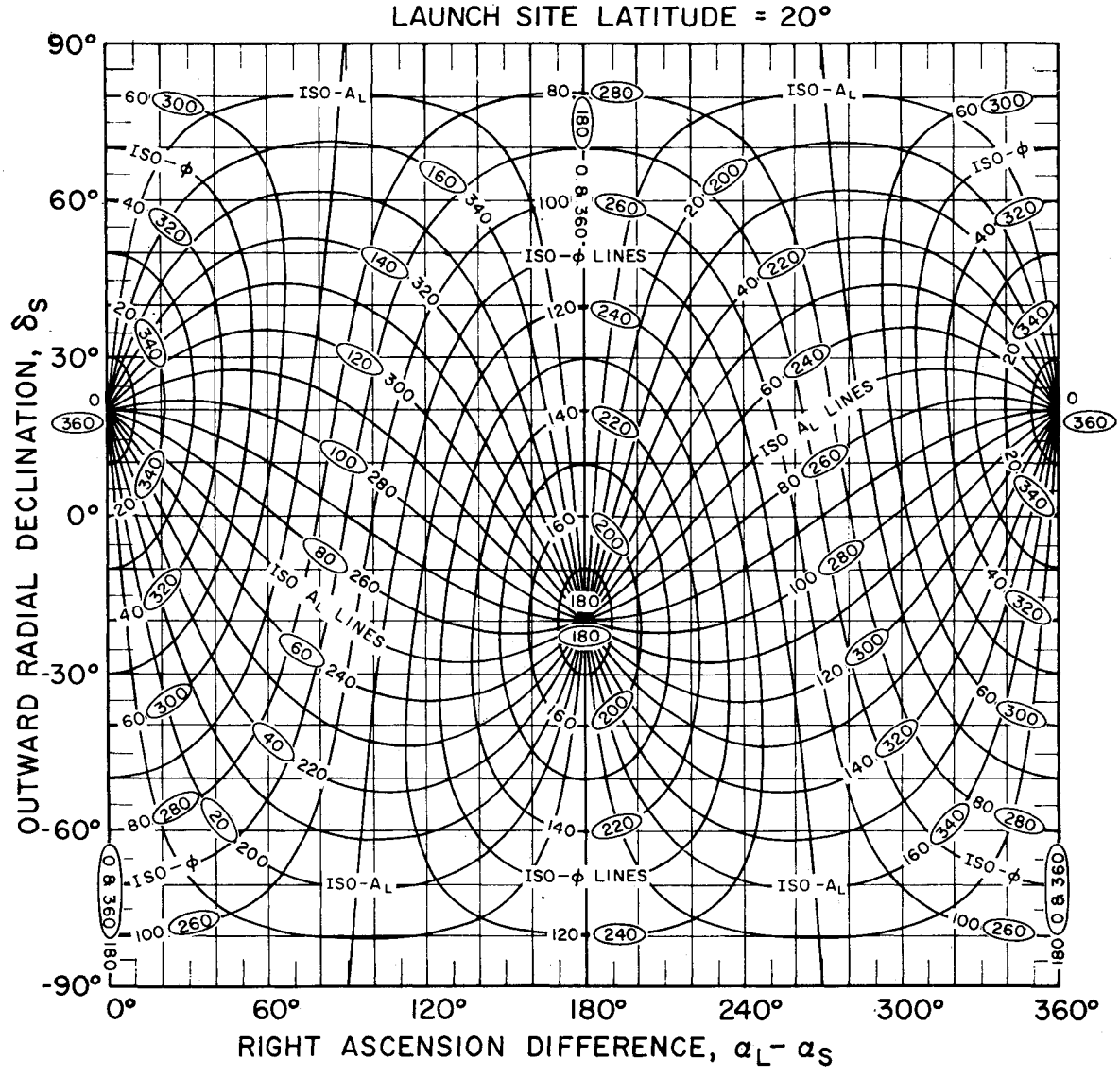

Fig. 7 Iso-φ and iso-A_L contours, 20°

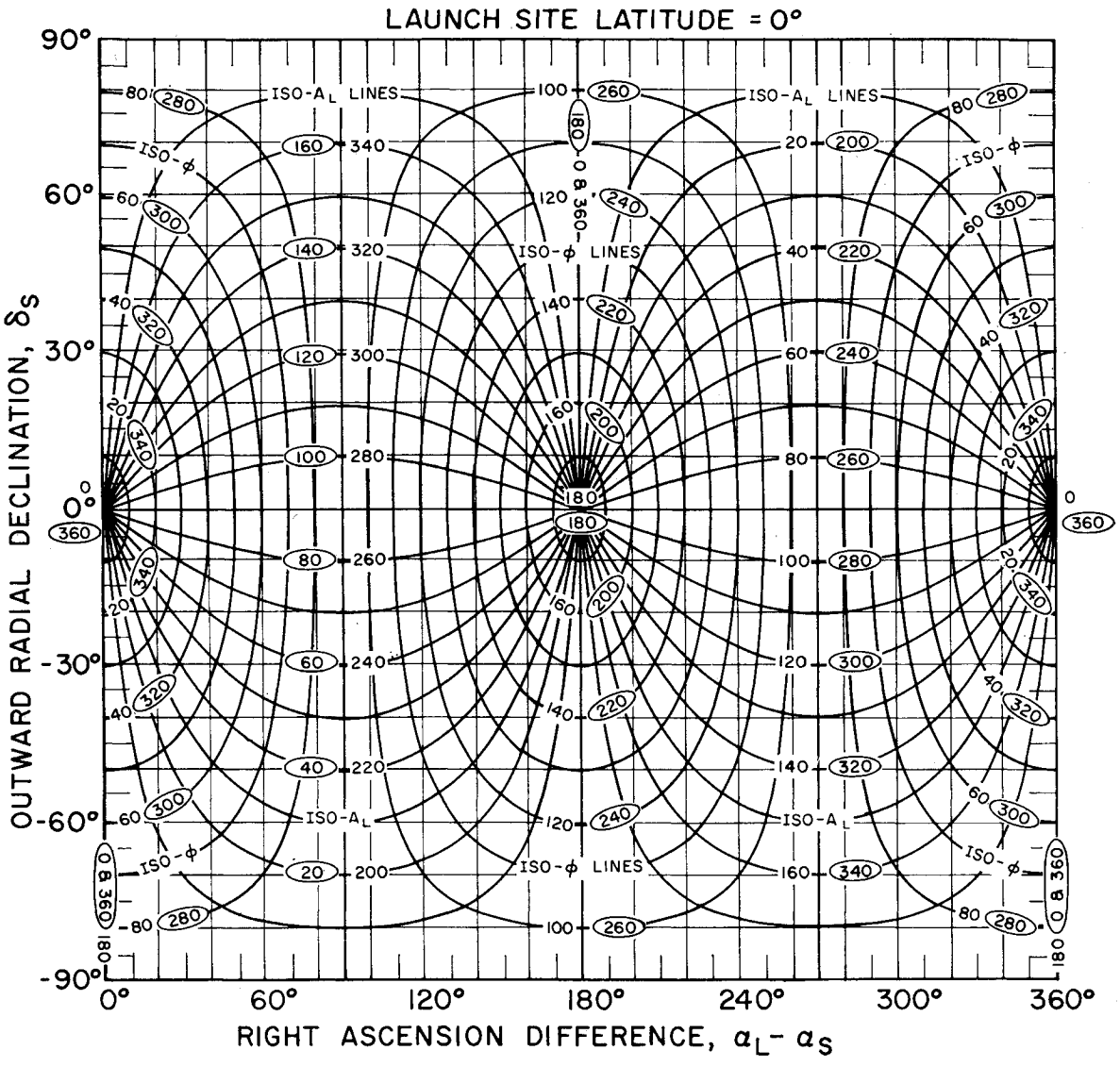

Fig. 8 Iso-φ and iso-A_L contours, 0°

and $\delta_s = -3^\circ.86$ (final values). Further iterations are not justified.

Summary of Results:

1) $A_L = 95°$, lunar arrival within $7^h.13$ of full phase:

AMR launch	$\alpha_L = 106^\circ.10$	$\varphi_p = 82^\circ.5$	$T_p = 0^h.44$
$12^h.44$ (September 21, 1961)	$\delta_L = 28^\circ.45$	$\varphi_b = 170°$	$T_b = 63^h.56$
		$\varphi = 252^\circ.5$	$T = 64^h.00$
Lunar arrival	$\alpha_s = 358^\circ.04$	100-naut-mile injection alt	$\gamma = 0°$
$4^h.44$ (September 24, 1961)	$\delta_s = -3^\circ.86$	$a \cong 53.35$ Earth radii	$V/V_{cir} \cong 1.40738$

and in a similar manner, one can determine the following:

2) $A_L = 110°$, lunar arrival within $5^h.44$ of full phase:

AMR launch	$\alpha_L = 131^\circ.62$	$\varphi_p = 61^\circ.5$	$T_p = 0^h.36$
$14^h.13$ (September 21, 1961)	$\delta_L = 28^\circ.45$	$\varphi_b = 170°$	$T_b = 63^h.64$
		$\varphi = 231^\circ.5$	$T = 64^h.00$
Lunar arrival	$\alpha_s = 359^\circ.04$	100-naut-mile injection alt	$\gamma = 0°$
$6^h.13$ (September 24, 1961)	$\delta_s = -3^\circ.39$	$a \cong 53.35$ Earth radii	$V/V_{cir} \cong 1.40738$

which gives a launch window $95° \leq A_L \leq 110°$ equal to $1^h.69$.

The results are an excellent first approximation for a precision lunar trajectory program search routine. Position and velocity vectors at injection may be calculated from these data for the particular coordinate system used in the precision program. In actual tests, the graphical results of this analysis have been accurate to within 0.20% of the actual injection velocity and to within 10 min of the correct launch time when the search has been performed on these parameters for perpendicular lunar impacts.

It should be noted that a trajectory timewise similar to that just mentioned could have been accomplished without using a parking orbit only during a few days in each month.

Referring to Fig. 2 and Ref. 8, one can determine that the $\varphi_{min} = 210°$ (for no parking orbit) is possible for $95° \leq A_L \leq 110°$ only when the lunar declination is negative 15°.25 or greater. This occurs in September 1961, for instance, between 2^h(September 16, 1961) and 10^h(September 21, 1961), an approximate $5\frac{1}{3}$-day period. Such lunar declinations coincide with lunar full phase conditions on May 30, June 28, and July 27 of 1961. Thus a "no-parking-orbit" launch could meet the lunar full phase constraint only during these three months. The use of parking orbits therefore can permit lunar launches at any time of the month and any month of the year, giving considerable flexibility to mission planning.

However, the biggest advantage of the parking orbit is its ability to ease the launch-on-time requirements for space missions in general.[6] As was demonstrated in the example, a launch time delay simply will rotate the launch azimuth angle and diminish the parking orbit coast. In practice, at the beginning of a day's launch window, the parking orbit coast would be determined for the smallest value of the launch azimuth angle to be used. Then if the launch were delayed for any reason, the parking orbit coast period simply would diminish with the Earth's timewise rotation until it vanished or until the permissible launch azimuth angle reached its maximum limit. Throughout a day's launch window of 1 or 2 hr, the point of injection essentially remains "fixed" in space, the only deviation being due to the small rotation of the flight plane.

For a given launch azimuth angle there are in general two possible launch times daily, one requiring a shorter parking orbit than the other. In most cases the shorter parking orbit would be used, but some tracking advantages sometimes may exist with the longer one depending upon the mission. The use of parking orbits has become and will continue to be a standard launch procedure for lunar and interplanetary missions.

6. Return Trajectories

The technique presented earlier in this paper can be used similarly in the selection of return trajectories by a simple reversal in time. A completely analogous situation exists between the pertinent parameters of launch and arrival. Thus, one "launches" to the moon backward in time from the return site back along the return azimuth and is "injected" into the transfer orbit at the re-entry flight path angle. Corresponding definitions of the various geometric and dynamic parameters are straightforward. Thus **L** is taken at Earth arrival and **S** at lunar launch. If the re-entry point is defined to be at the same altitude as injection (100 naut miles) and the latitude of the return point is the same as AMR, the same curves of Figs. 2 and 5 may be used to select return trajectories for any arrival longitude θ_L. Of course the dynamics of re-entry differ from those of boost, but the resulting parameters γ, φ_p, T_p, and V have equivalent functions. If an Earth arrival is desired at latitudes different from AMR, the curves of Fig. 2 merely have to be replaced with others applicable to the desired latitude. An example of such "return" curves are presented in Figs. 7 and 8 for return latitudes of 20° and 0°, respectively.

As with outgoing trajectories, return trajectories will be subject to certain constraints, the most important of which are probably Earth re-entry conditions. The arrival azimuth angle would depend upon choice of arrival site and possible local tracking facilities. These are handled easily by the technique presented herein. The tracking constraint would most likely require a lunar launch during a visibility window from a station with command capability. For a lunar soil sample return such as had been proposed for the Prospector mission, a dawn Earth arrival constraint might be imposed to allow a maximum of daylight hours for search in the event that contact with the re-entering vehicle is lost. Furthermore, such a return flight would have to be "matched" to an outward flight, with a lunar "stay period" of 24 to 48 hr sandwiched between, sufficient for the lunar sample acquisition. Flight times would depend on lunar launch requirements (injection velocity vector) and upon probably injection guidance errors.

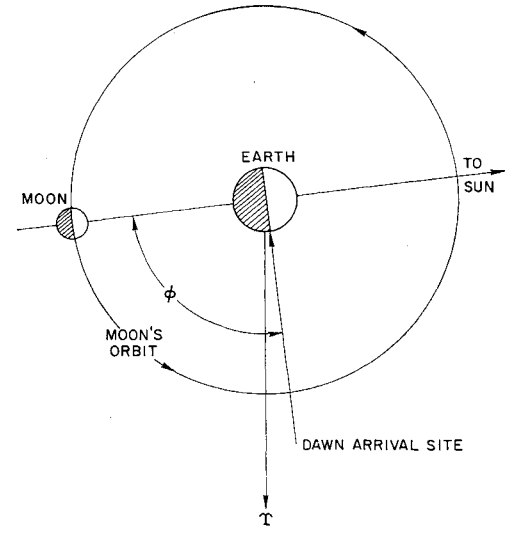

Fig. 9 Geometry for direct return with dawn earth arrival

A dawn Earth arrival requirement specifies the relationship of the arrival site to the sun's position at the arrival time. For a re-entry angle (unmanned) of, say −40° at 100-naut-mile alt, the ballistic central angle φ_b ranges in value between 88° and 99° for trip times of 50 and 100 hr, respectively (see Fig. 5). Therefore, the angular relationship between a dawn Earth arrival site and the moon's position at launch requires that direct return trajectories be launched when the moon is close to its full phase or 88° to 99° (plus re-entry central angle) behind the arrival site. This is illustrated in Fig. 9. By similar reasoning a retrograde return, for a −40° re-entry angle would place the moon 88° to 99° (plus re-entry central angle) ahead of the arrival site or close to its new phase.

In the example that follows it is assumed that constraints of this type have been specified. The problem again is to select a compatible return trajectory that can be used as a first approximation to a precision trajectory search program in which the time reversal technique can be employed, i.e., the program can be run backward in time.

Example II: Lunar Return Trajectory

Given:

1) Earth arrival site—Edwards Air Force Base (latitude approximately the same as PMR, longitude 117°.8 W).
2) $180° \leq A_L \leq 360°$† (direct return).
3) $T_p = 0^h.01$ (feasible unHanned re-entry value).
4) $\varphi_p = 1°$ (feasible unmanned re-entry value).
5) $\gamma = 40°$ (feasible unmanned re-entry value).
6) $r_1 = 4078$ statute miles (100-naut-mile alt).
7) $50^h \leq T \leq 100^h$ (select two possible return times within T range).
8) Lunar launch with Goldstone visibility.
9) Earth arrival at approximately dawn.
10) Return "matched" to ascent trajectory of Example I after an approximate 24-hr lunar stay.

Solution:

1) Lunar arrival for the ascent trajectory of Example I was between $4^h.44$ to $6^h.13$ (September 24, 1961) and had Gold-

† A_L for return trajectories refers to the direction from which the vehicle is approaching the arrival site to be consistent with the time reversal concept.

stone visibility. After about a 24 hr stay, a return launch at 5^h (September 25, 1961) would also have Goldstone visibility.

2) From Ref. 8 (p. 134) for a lunar launch at 5^h (September 25, 1961) read $\alpha_s = 12.^\circ44$ and $\delta_s = +1.^\circ33$.

3) From Fig. 5, for $\gamma = 40^\circ$ and a first guess for $T_b = 50^h$ read $\varphi_b = 88.^\circ5$.

4) $\varphi = \varphi_p + \varphi_b = 1^\circ + 88.^\circ5 = 89.^\circ5$.

5) From Fig. 3, for $\delta_s = +1.^\circ33$ and $\varphi = 89.^\circ5$ read $(\alpha_L - \alpha_s) = 91^\circ$ with $A_L = 272^\circ$ (direct) or $(\alpha_L - \alpha_s) = 269^\circ$ with $A_L = 88^\circ$ (retrograde). Select the "direct" return and proceed.

6) Compute: $\alpha_L = (\alpha_L - \alpha_s) + \alpha_s = 91^\circ + 12.^\circ44 = 103.^\circ44$.

7) From Ref. 8 (p. 15) for 0^h (September 27, 1961), the day of arrival, read GHA $= 5.^\circ55$.

8) Compute: $t_L = (\alpha_L - \text{GHA} - \theta_L)/\omega = [103.^\circ44 - 5.^\circ55 - (-117.^\circ8)]/15.^\circ04107 = 14.^h34$ (September 27, 1961) arrival time.

9) Compute: $T = 14.^h34$ (September 27, 1961) $- 5^h$ (September 25, 1961) $= 57.^h34$.

10) $T_b = T - T_p = 57.^h34 - 0.^h01 = 57.^h33$.

11) Again from Fig. 5, for $\gamma = 40^\circ$ and $T_b = 57.^h33$ read $\varphi_b = 91^\circ$.

12) $\varphi = \varphi_p + \varphi_b = 1^\circ + 91^\circ = 92^\circ$.

13) Again from Fig. 3, for $\delta_s = +1.^\circ33$ and $\varphi = 92^\circ$, read $(\alpha_L - \alpha_s) = 94^\circ$ with $A_L = 273^\circ$ (direct).

14) Recompute: $\alpha_L = 94^\circ + 12.^\circ44 = 106.^\circ44$, $t_L = [106.^\circ44 - 5.^\circ55 - (-117.^\circ8)]/15.^\circ04107 = 14.^h54$ (September 27, 1961), $T = 14.^h54$ (September 27, 1961) $- 5^h$ (September 25, 1961) $= 57.^h54$, and $T_b = 57.^h54 - 0.^h01 = 57.^h53$.

15) Finally, from Fig. 5, for $\gamma = 40^\circ$ and $T_b = 57.^h53$, read $\varphi_b = 91^\circ$ with no further iterations required.

16) Final Earth arrival date-time $= 14.^h54$ (September 27, 1961). Universal time is the local mean solar time at the Greenwich meridan. The local mean solar time at arrival site is $117.^\circ8/15 = 7.^h85$ earlier or 6:41 a.m. From Ref. 8 (p. 390), the local mean solar time of sunrise on September 27, 1961 is 5:51 a.m. or 50 min earlier.

Summary of Results:

Lunar launch $5.^h00$ (September 25, 1961): $\alpha_s = 12.^\circ44$, $\delta_s = +1.^\circ33$; 100-naut-mile re-entry alt, $\gamma = -40^\circ$

$T = 57.^h54$, Earth arrival at 6:41 a.m. local mean solar time

(50 min after local dawn)

Earth arrival $14.^h54$ (September 27, 1961)				
$\alpha_L = 106.^\circ44$	$\varphi_p = 1^\circ$	$T_p = 0.^h01$		
$\delta_L = 34.^\circ8$	$\varphi_b = 91^\circ$	$T_b = 57.^h53$		
	$\varphi = 92^\circ$	$T = 57.^h54$		
$A_L = 273^\circ$	$a \cong 80.91$ Earth radii	$V/V_{cir} \cong 1.40956$		

and in like manner, for a flight time roughly 24^h longer $T = 81.^h81$, Earth arrival at 6:58 a.m. local mean solar time

(66 min after local dawn)

Earth arrival $14.^h81$ (September 28, 1961)				
$\alpha_L = 111.^\circ44$	$\varphi_p = 1^\circ$	$T_p = 0.^h01$		
$\delta_L = 34.^\circ8$	$\varphi_b = 95^\circ$	$T_b = 81.^h80$		
	$\varphi = 96^\circ$	$T = 81.^h81$		
$A_L = 276^\circ$	$a \cong 34.47$ Earth radii	$V/V_{cir} \cong 1.40361$		

Another return flight time 24^h greater than the last (approx 106^h) also would be possible having the same lunar launch time but arriving at Earth one day later. If the return azimuth A_L had been constrained to some particular value, it is obvious from Fig. 3 that the dawn Earth arrival constraint could not be maintained. The effects of other constraints in input conditions become manifest as one examines the graphical relationships of the curves and attempts to satisfy them.

The return trajectories previously obtained are defined in terms of Earth arrival parameters rather than those at lunar injection which may impose problems in trying to reproduce them on a precision trajectory computer program. However, if the precision program is capable of running timewise backward, the problem is practically the same as with ascent trajectories. Using the data from the example as a "first approximation," the vehicle is "injected" backward to the moon at the arrival time with re-entry conditions. The precision program is then run backward in time, such that the vehicle "arrives" in the vicinity of the moon at the launch time. The same search routines that were used in regular ascent trajectories then can be used to converge upon the desired lunar injection position and launch time. Thus exact lunar injection data is obtained and the return trajectory then can be rerun in the normal fashion from moon to Earth with re-entry and arrival conditions at Earth assured. This is a distinct advantage since re-entry conditions are basic to the design of the re-entry vehicle and impose constraints that are difficult to handle if the return trajectory were defined only by launching parameters at the moon.

References

[1] Lieske, H. A., "Lunar trajectory studies," Rand Corp. Paper 1293 (February 26, 1958).

[2] Micklewait, A. B. and Booton, R. C., "Analytical and numerical studies of three-dimensional trajectories to the moon," IAS Paper 59-90 (June 1959).

[3] Michael, W. H. J. and Crenshaw, J. W., "Trajectory considerations for circumlunar missions," IAS Paper 61-35 (January 1961).

[4] Nelson, W. C., "An integrated approach to the determination and selection of lunar trajectories," J. Astronaut. Sci. **8**, 33–39 (1961).

[5] Clarke, V. C., Jr., "Design of lunar and interplanetary ascent trajectories," Jet Propulsion Lab. TR 32-30 (July 1960).

[6] Kohlhase, C. E., "Launch on time analysis for space missions," Jet Propulsion Lab. TR 32-29 (August 1960).

[7] Vertregt, M., "Interplanetary orbits," J. Brit. Interplanet. Soc. **16**, no. 6, 326–354 (1958).

[8] *The American Ephemeris and Nautical Almanac for 1961* (U. S. Government Printing Office, Washington, D. C., 1959).